18TH WORLD CONFERENCE ON EARTHQUAKE ENGINEERING
WCEE2024
MILAN

MILAN, ITALY
30TH JUNE - 5TH JULY 2024
www.wcee2024.it

A BNWF APPROACH TO ASSESS THE RESPONSE OF SINGLE PILE SUBJECTED TO FAR-FIELD AND NEAR-FIELD GROUND MOTIONS

B. E. Ajom[1], K. Dasgupta[2] & A. Dey[2]

[1] Indian Institute of Technology Guwahati, Guwahati, India, begum176104101@iitg.ac.in

[2] Indian Institute of Technology Guwahati, Guwahati, India

Abstract: *Kinematic responses of single fixed-head vertical piles in homogeneous loose sand profile under far-field and near-field ground motions have been studied. For numerical simulation of soil-pile interaction, Beam on Nonlinear Winkler Foundation (BNWF) modelling technique has been adopted. The soil and pile behaviours are represented using nonlinear Winkler springs and beam-column elements, respectively. The Winkler springs are modelled using a series of p–y, t-z and Q-z curves to represent the lateral and axial soil–pile interaction. To obtain the free-field earthquake motions for application at the free ends of the nonlinear p-y springs along the depth of the pile, nonlinear site response analyses have been carried out separately. This study focuses on assessing the impact of ground motion characteristics, longitudinal reinforcement percentages and pile diameter on the nonlinear response of piles. The response of a single pile has been studied considering the minimum and maximum reinforcement criteria recommended by the relevant Indian Codes of Practice. The outcomes of the study are presented in terms of maximum bending moments of the pile, stress-strain histories of the pile material and plastic hinge lengths.*

1. Introduction

During an earthquake, the dynamic forces transmitted to the foundation can induce significant deformations and stresses in the pile-soil system. Depending on the characteristics of the ground motion, soil properties, and pile configuration, nonlinear behaviour can manifest in the piles themselves. This may include plastic deformations, changes in lateral stiffness, and degradation of load-carrying capacity. The nonlinear response of piles under strong ground motions can result from various factors, such as soil-pile interaction, pile material properties, and the structural detailing of the pile. The dynamic forces can cause pile bending, axial loading, and shear forces that can lead to inelastic deformations and energy dissipation within the pile.

For a pile foundation subjected to severe earthquakes, the key mechanism to attain ductile performance solely involves development of plastic hinges along the pile length. While designing a pile, it is important to have prior knowledge of both the location and size of the plastic hinge zone to estimate confinement in the plastic hinge region. Song et al. (2005) in their study, elaborated the response of a fixed-head pile for various limit states. Under significant lateral loading, a fixed-head pile undergoes sequential yielding until a plastic mechanism is fully developed as depicted in Figure 1. The first yield limit state of the pile is characterised by the maximum Bending Moment (BM) developed at any location along the length of the pile (including the pile-pile cap connection region) where the yield flexural strength M_u of the pile is reached. As a result, a plastic hinge is assumed to develop at that location. Figure 1a shows the formation of plastic hinge at the top of the pile with the centre of rotation occurring at the ground level. With increasing displacement, redistribution of internal

forces takes place leading to an increase in BM in the non-yielding portion of the pile thereby forming a second plastic hinge at a depth L_m as shown in Figure 1(b). After the formation of the second plastic hinge, when the pile experiences further displacement, large inelastic rotations occur at both the plastic hinges until the pile reaches the ultimate limit state, as shown in Figure 1(c). Several studies have been conducted to estimate the equivalent plastic hinge length of extended pile-shafts (Budek et al., 2000; Chai, 2002; Heidari and Naggar, 2018). The analytical methods used to estimate plastic hinge length are established based on static lateral loading protocol applied at the pile head. However, the present study specifically focuses on observing the plastic hinge zone of single piles under seismic loading conditions.

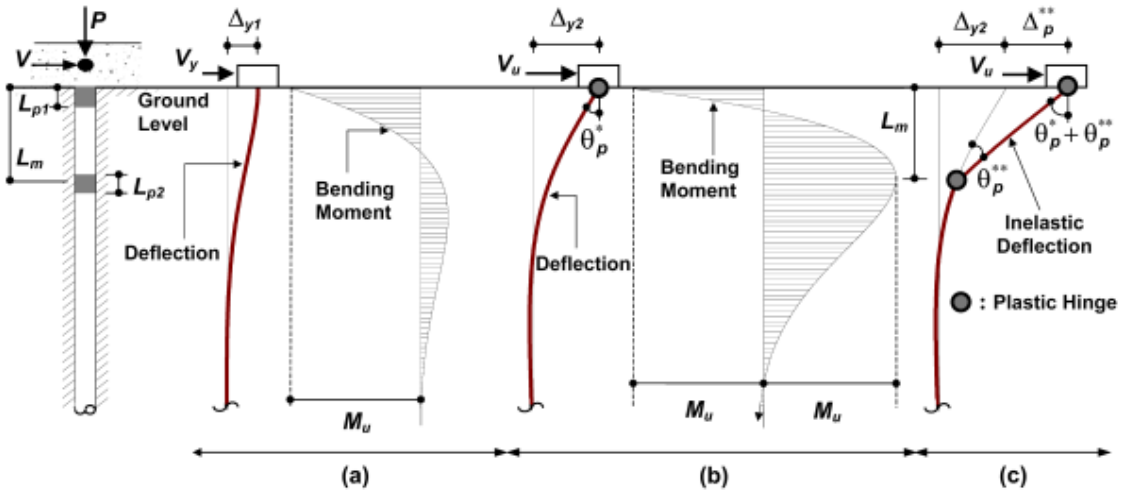

Figure 1. Deflected shape and bending moment distribution of a laterally loaded fixed-head pile (a) first yield limit state, (b) second yield limit state, and (c) ultimate limit state (Song et al., 2005).

2. Ground motion selection

In this study, a suite of total nine ground motions is considered with different duration and frequency content, comprising both far-field and near-field earthquakes from a variety of tectonic environments, selected from the Pacific Earthquake Engineering Research Center (PEER) ground motion database. The selection of these ground motions is based on specific criteria related to the earthquake magnitude (M) and the distance (R) of the rupture zone from the site. These motions are used as bedrock motion for the site response analyses.

Near-field earthquakes release a large portion of fault energy in the form of pulses. Pulses can normally be recognized through acceleration, velocity, and displacement time histories. Near-field earthquake ground motions have higher acceleration and more limited frequencies as compared to the higher frequency contents of ground motions from far-field earthquakes. Far-field earthquakes typically have larger epicentral distances, and their effects at the site are primarily governed by the propagation of seismic waves through the earth's crust. Although established guidelines are absent regarding the limiting epicentral distance for near field earthquakes, currently, an epicentral distance less than 12 km is taken as the criterion for choosing the near-field range as per Chopra and Chintanapakdee (2001).

A set of five far-field and four near-field ground motions used in this study are listed in Table 1. The earthquakes range in magnitudes from 5.8 to 7.63. The acceleration time histories of the far-field and near-field ground motions are shown in Figure 2(a). The Peak Horizontal Accelerations (PHA) of the far-field earthquakes are less than that of the near-field earthquakes. The mean spectrum of the far-field and near-field ground motions is shown in Figure 2(b). As seen from the figure, the mean spectral response of the near-field ground motions is significantly greater than that of their far-field counterparts.

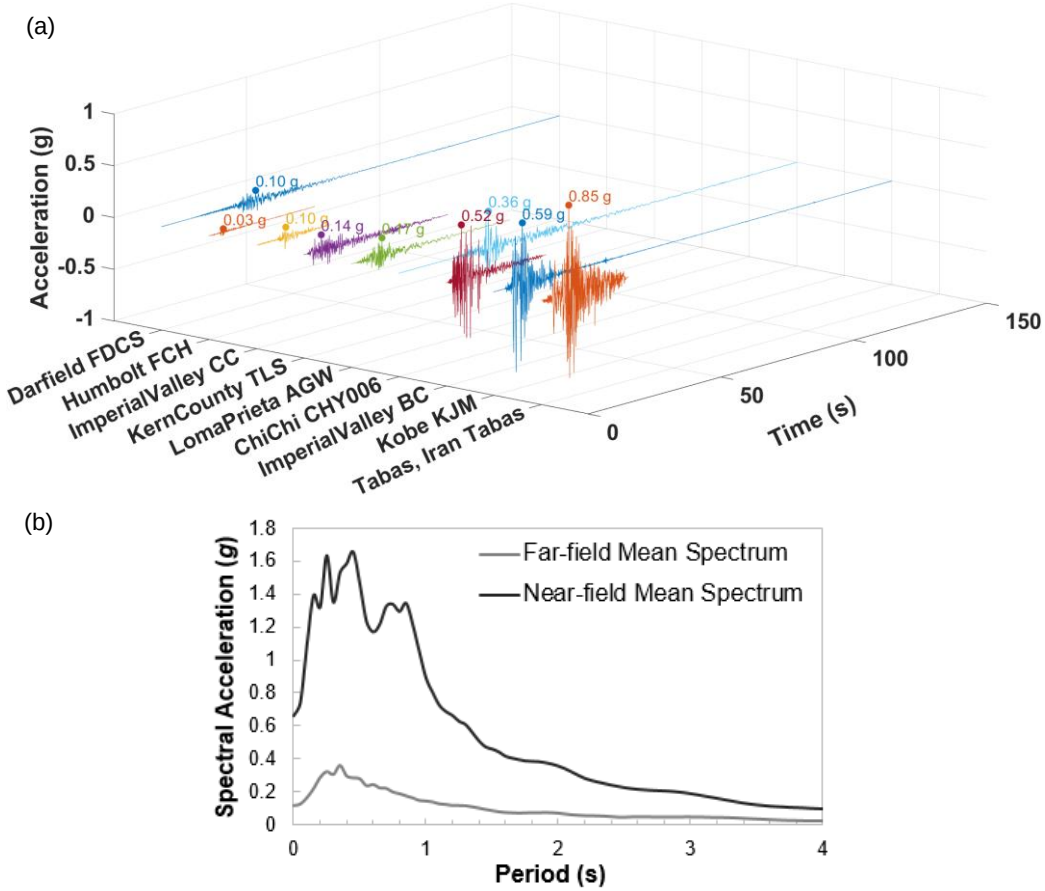

Figure 2. (a) Acceleration time histories and (b) Mean spectrum; of the far-field and near-field ground motions.

Table 1. Ground motion parameters for the selected earthquakes

	No.	Earthquakes	Year	Station	Distance (km)	Comp.	M	PHA (g)	PHV (cm/sec)
Far-field motions	1	Darfield	2010	FDCS	91.59	NW	7.0	0.102	13.31
	2	Humbolt Bay	1937	Ferndale City Hall	71.57	225	5.8	0.036	2.36
	3	Imperial Valley	1979	Coachella Canal	50.1	045	6.53	0.116	12.83
	4	Kern County	1952	Taft Lincoln School	38.89	021	7.63	0.159	15.22
	5	Loma Prieta	1989	Agnews State Hosp.	24.57	000	6.93	0.169	33.50
Near-field motions	6	Chi-Chi	1999	CHY006	9.76	N	7.62	0.355	42.32
	7	Imperial Valley	1979	Bonds Corner	2.66	140	6.53	0.594	46.73
	8	Kobe	1995	KJMA	0.96	000	6.9	0.834	91.07
	9	Tabas, Iran	1978	Tabas	2.05	Longi.	7.35	0.854	98.81

PHA = Peak Horizontal Acceleration; PHV = Peak Horizontal Velocity

3. Pile-soil interaction analysis with BNWF model

The nonlinear single pile analysis conducted for this research using the BNWF technique comprises of two steps. Firstly, a nonlinear site response analysis is carried out to determine the free-field motions within the soil deposit. Secondly, the pile-soil interaction is evaluated using a BNWF model where the pile is connected to a series of nonlinear soil springs and the free-field displacement time histories at each depth obtained from the site response analysis are applied to the free ends of the lateral springs as an excitation to the system.

3.1 Site response analysis

Different sites have unique soil profiles and geological conditions, leading to site-specific ground response characteristics. Site response analysis allows for the consideration of these site-specific factors, ensuring accurate modeling and representation of the free-field motions. One-dimensional nonlinear site response analysis has been carried out using OpenSees (McKenna, 2011). The soil is modeled in two-dimensions as a soil column using the plane strain formulation of the quad element. A general schematic of the model is shown in Figure 3. To simulate the nonlinear hysteretic response of soil materials, advanced constitutive models are employed. Absorbing boundaries are employed at the base of the soil column to account for the finite rigidity of the underlying bedrock. Subsequently, the soil column is dynamically excited at the base by a horizontal force time history which is proportional to the velocity time history of the ground motion. The displacement time histories at various depths are recorded, and these recorded time histories are subsequently utilized as input for the BNWF model.

To perform the site response analysis for the parametric study, loose sand subjected to nine different ground motions is taken into account, the mass density (ρ) and the angle of internal friction (φ) of which are considered as 1.7 t/m^3 and 29°, respectively. The shear wave velocity of the homogeneous sandy soil profile is taken as 180 m/s.

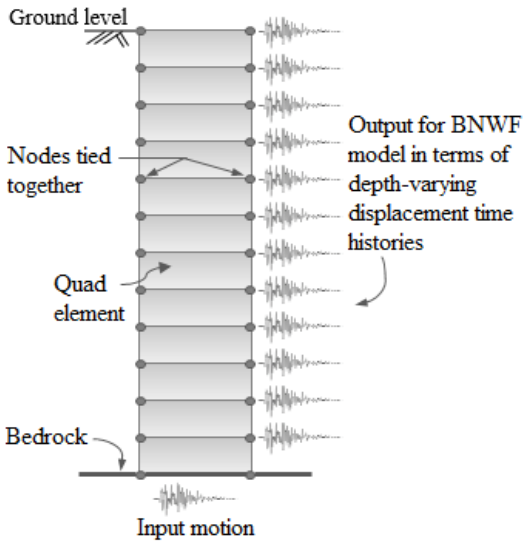

Figure 3. Schematic representation of free-field soil-response model.

3.2 Modelling of soil-pile interaction

In this study, the soil-pile interaction is simulated in OpenSees as a BNWF model using displacement-based beam-column elements to represent the pile and the soil is represented through a series of discrete nonlinear macro-elements that consist of springs and dashpots. For the lateral soil-pile interaction, the nonlinear behaviour is characterized as consisting of visco-elastic, plastic and gap components in series (Boulanger et al. 1999). The plastic component is simulated by developing a relationship between the lateral pile deflection, y, and the soil resistance, p, known as the $p-y$ curve. Similarly, the nonlinear behaviour of the axial resistance of the pile along the pile shaft and the end bearing resistance at the pile tip is conceptualized using the visco-elastic and plastic components in series. $t-z$ and $Q-z$ curves are then used to simulate the plastic components of the respective macro-elements. These macro-elements, also known as soil springs in simple terms, are generated using zero-length elements each consisting of two nodes sharing the same location. The pile is discretized into 0.5 m long beam elements and the nonlinear springs are attached to each pile node at one end and are applied with displacement time histories at the other for conducting the dynamic analyses. Based on a separate study, it was found that the element length of 0.5 m gives a satisfactory level of accuracy and hence the element length has been kept constant throughout this study. A schematic of the dynamic BNWF model is presented in Figure 4.

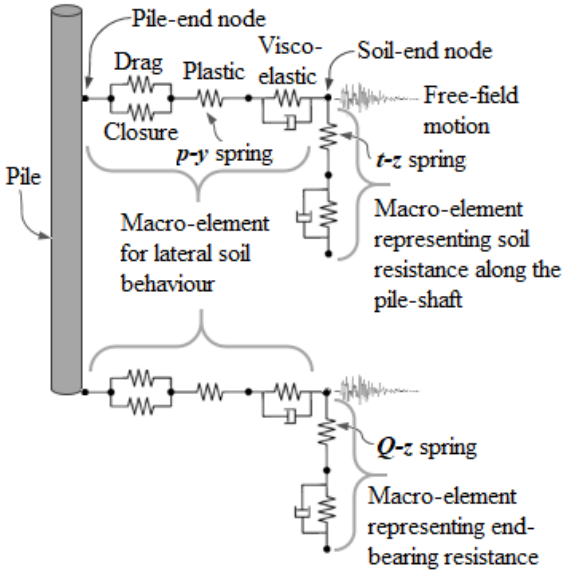

Figure 4. Schematic representation of a spring-dashpot-pile model.

In the present study, API (2000) recommendations have been considered for characterizing soil springs. For sandy soil, the model of Murchison and O'Neill (1984) is used to find the ultimate lateral bearing capacity (p_u). The lateral soil resistance-deflection ($p-y$) non-linear relationships for sand at any specific depth H, is calculated using the following equation:

$$p = A \times p_u \times \tanh\left[\frac{k \times H}{A \times p_u} \times y\right] \quad (1)$$

where, A is a factor accounting for cyclic or static loading condition; k is the initial modulus of subgrade reaction in kN/m^3 and y is the lateral deflection in m.

The fibre-based technique is adopted to model the nonlinear response of the reinforced concrete (RC) piles. In this well-known approach, the cross-section of the RC member is divided into a number of small segments called fibres. The fibres are then assigned with the respective constitutive materials to represent the cover concrete, core concrete and the longitudinal steel reinforcement in the RC section. In this study, the fibres of core and cover concrete are modelled using Kent-Scott-Park model (Scott et al., 1982) and that of longitudinal reinforcing bars using Giuffre-Menegotto-Pinto (Filippou et al., 1983) material model. The confined concrete properties have been obtained from the relation proposed by Park et al. (1982) and Scott et al. (1982). To enhance the strength and ductility of concrete due to the confinement effects, a factor K has been multiplied to the peak strength and the corresponding strain of the concrete where $K = 1.25\left(1 + \frac{\rho_s f_{yh}}{f_c'}\right)$ in which ρ_s is the ratio of volume of hoop reinforcement to volume of concrete core measured to the outside of the hoops, f_{yh} is the yield strength of hoop or transverse reinforcement and f_c' is the characteristic compressive strength of concrete. Also, to calculate the maximum concrete compressive strain for confined concrete, the following equation suggested by Scott et al. (1982) has been utilized.

$$\varepsilon_{cu} = 0.004 + 0.9\rho_s\left[\frac{f_{yh}}{300}\right] \quad (2)$$

4. Validation study

The validity of the dynamic BNWF approach in predicting seismic response of a single pile is assessed by simulating a centrifuge test (No. 12) conducted by Gohl (1991) on a steel pipe pile in a homogeneous sandy soil profile (Figure 5). Seismic soil-pile interaction analysis of the experimental centrifuge test has been performed using the methodology described above. A horizontal acceleration record with a peak acceleration of 0.15 g is given as the input at the base of the system. Displacement-time histories at different depths are

extracted from the free-field site response analysis and are applied as input motion to soil-end nodes of the springs.

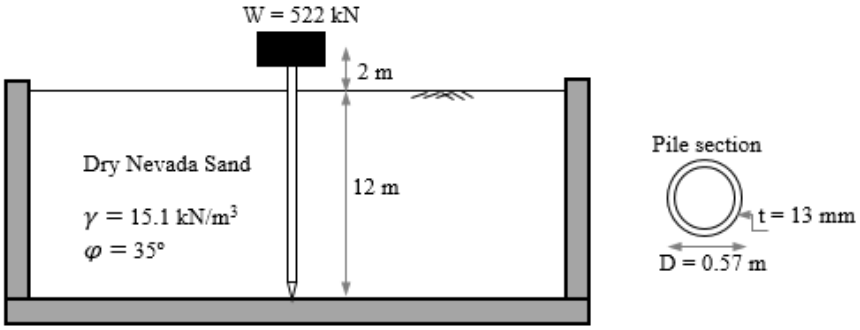

Figure 5. Prototype model of the single pile centrifuge test of Gohl (1991)

Figure 6(a) compares the spectral response of the free-field motions at the ground surface derived from the numerical result from site response analysis to that of the centrifuge test -- a good agreement is observed between the experimental and numerical results. Figure 6(b) shows the acceleration response spectra of the pile-head motions extracted from the numerical result of the BNWF model to that of the centrifuge test. The figure illustrates that the numerical simulation yields a stiffer response, reaching its peak slightly earlier at 0.9 seconds, in contrast to the experimental data, which reaches its peak at 1 second. Additionally, the spectral acceleration peak value of the pile head slightly overestimates the experimental results. However, overall, there is a good match between the numerical and experimental results for both soil and pile responses.

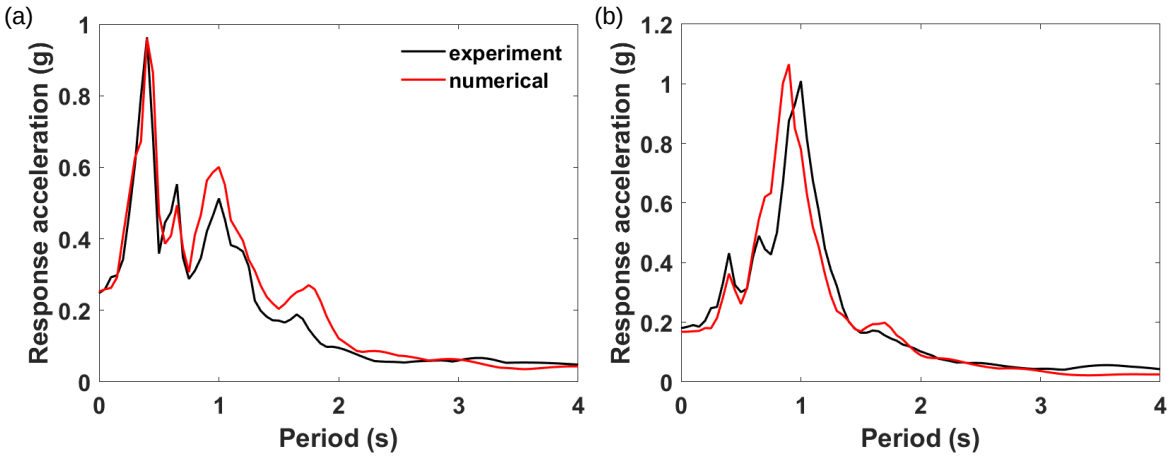

Figure 6. Acceleration response spectra comparing the measured responses of (a) free-field motion at ground surface and (b) pile-head motion, from the centrifuge test with the numerical results.

5. Parametric investigation

Design of piles has been carried out in accordance with IS 2911-1-2 (2010), IS 456 (2000), SP 16 (1980), and IRC 112 (2011). Bored cast in-situ RC piles which are the most commonly used piles are considered for this study. The length of the piles has been determined using the long pile criteria specified in Annex C of IS 2911-1-2 (2010). According to Clause 6.11.1 of this code, the minimum area of longitudinal reinforcement within the pile shaft shall not be less than 0.4% of the cross-sectional area of the pile shaft. It is a common practice for designers to consider the minimum reinforcement criteria for pile reinforcement when designing piles. Therefore, in this study, the percentages of longitudinal reinforcement are varied (0.4%, 1%, 2% and 4%) to investigate the effects on the behaviour and nonlinearity of the piles. The transverse reinforcements are provided in accordance with the guidelines of IRC 112 (2011) to confirm the ductility of the piles.

Performance of 25 m long, single fixed-head floating pile with circular cross-section is investigated with the diameters of the piles as 0.7 m and 1.2 m, respectively. As the present study is focused on the kinematic interaction of the piles, no axial load or inertial load coming from the superstructure is considered at the pile head. The grade of concrete is considered as 40 MPa and the grades of longitudinal and transverse

reinforcements are considered as 500 MPa and 250 MPa, respectively. Diameters of the longitudinal and transverse bars are considered as 20 mm and 10 mm respectively. It is assumed that the pile head is positioned at ground level and is fully restrained, emulating a scenario where the pile is monolithically connected to a pile cap.

6. Results

The responses of the single piles are presented in the form of maximum BMs, material stress-strain histories and plastic hinge lengths along with the variation of longitudinal percentages. The influence of ground motion characteristics such as near-field and far-field earthquakes and PHAs are studied considering nine strong ground motions. Also, the study investigates the formation of plastic hinges on the piles under earthquake loading and presents important observations based on the findings.

6.1 Influence of ground motion characteristics

Figure 7 represents the histogram of the maximum BMs with the variation of longitudinal reinforcement percentages in the single piles of diameter 1.2 m under nine far-field and near-field ground motions. It is expected that the maximum BMs of the piles under far-field earthquakes with lower PHAs would be comparatively lesser, while those for near-field earthquakes with higher PHAs would be higher. Although the observations show a similar trend, for the Loma Prieta earthquake, which is categorized as a far-field earthquake with lesser PHA, the maximum BMs for all the four longitudinal reinforcement percentages are nearly similar to the maximum BMs observed under the near-field earthquakes.

This discrepancy might be due to the method used in this study to classify ground motions as far-field or near-field, which relies solely on the epicentral distance. Baker (2007) suggested that earthquakes with an original ground motion peak velocity exceeding 30 cm/sec are considered as near-field earthquakes. From Table 1, it is evident that the peak velocity of the Loma Prieta earthquake surpasses the 30 cm/sec threshold and hence falls in the category of near-field earthquakes.

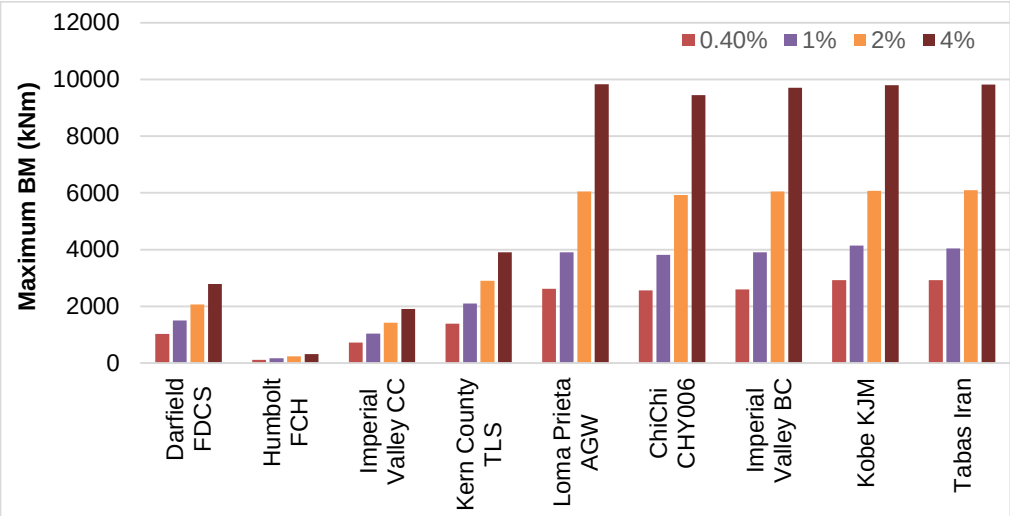

Figure 7. Histogram representing the maximum bending moment with the variation of longitudinal reinforcement percentages in the single piles of diameter 1.2m under nine far-field and near-field ground motions.

6.2 Material stress-strain behaviour

Figure 8 depicts the maximum stress-strain responses of the cover concrete, core concrete and reinforcing steel for the 1.2 m diameter pile with 0.4% longitudinal reinforcement under Imperial Valley BC and Kern County TLS earthquakes which are a near-field and a far-field earthquake, respectively. Under the ground motions of those earthquakes, cover concrete attains its peak strength; however, it undergoes more strain in case of the near-field earthquake as compared to the far-field one. While on the contrary, core concrete reaches its ultimate strength in case of the near-field earthquake, undergoing a higher strain than it does during the far-field earthquake, where it fails to achieve its maximum strength. This trend is also observed in the reinforcing steel, which experiences greater strain during the near-field earthquake in contrast to the far-field

one. The differences in strain response among these materials indicate varying levels of stress and strain intensity based on the proximity of the earthquake.

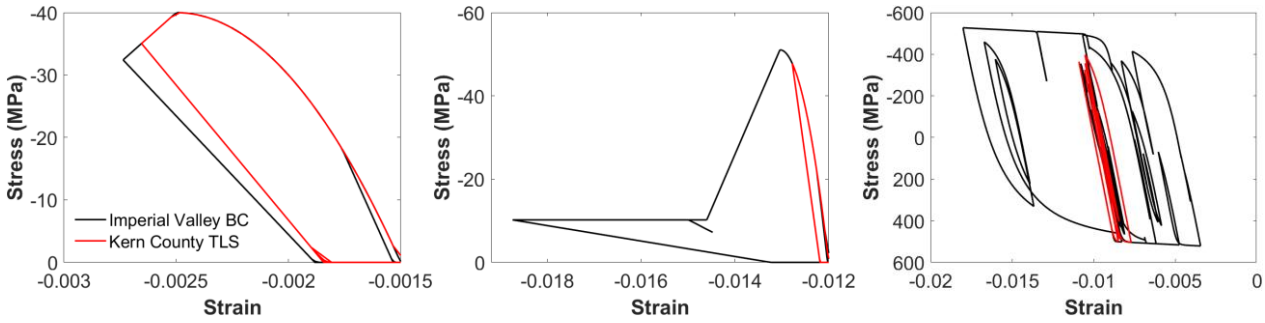

Figure 8. Maximum stress-strain histories for (a) cover concrete (b) core concrete and (c) reinforcing steel for the 1.2m diameter pile with 0.4% longitudinal reinforcement under a near-field and a far-field earthquake.

6.3 Plastic Hinges

As the BM reaches the yield moment of the pile cross section, M_y, a plastic hinge develops, at which point the curvature reaches the yield value. This concept has been used in this study to determine the plastic hinge length (L_p) of the pile. The moment-curvature analyses of the pile section were carried out for four different variations in longitudinal reinforcement percentages to find the yield moment of each pile section. The yield moment which represents the BM of the pile at the first yield of the extreme fibre reinforcement is estimated to be 655 kNm, 1653 kNm, 3331 kNm and 6308 kNm for longitudinal reinforcement percentages of 0.4%, 1%, 2% and 4%, respectively, for the 1.2 m diameter pile. Whereas, for the 0.7 m diameter pile the yield moments were 848 kNm and 1657 kNm for 2% and 4% longitudinal reinforcement percentages, respectively.

Plastic hinge zone

Figures 9(a), 9(b), 9(c) and 9(d) show the maximum BM profiles of the 1.2 m diameter pile under nine ground motions for four variation of longitudinal reinforcement percentages. These plots depict the maximum BMs of the pile crossing the yield moment along the pile length. For 0.4% and 1% longitudinal reinforcement, plastic hinges are observed at two distinct zones: near the pile-head, where maximum BM occurs, and at a location with a local maximum BM in the reverse direction. This trend is consistent for all near-field earthquakes and for the Loma Prieta earthquake among the far-field earthquakes. However, for other far-field earthquakes with lesser PHAs, plastic hinges are observed only near the pile-head.

In contrast, for 2% and 4% longitudinal reinforcement, plastic hinges are observed to form only near the pile-head under near-field and Loma Prieta earthquakes. Under other far-field earthquakes having lesser PHAs, plastic hinges were observed for 0.4% and 1% longitudinal reinforcement near the pile-head, while no plastic hinges develop for 2% and 4% longitudinal reinforcement. Specifically, for the Humbolt earthquake characterized by the lowest PHA of 0.036 g among all the nine earthquakes, there was a notable absence of plastic hinge formation across the entire length of the pile.

Similarly, the maximum BM profiles of the 0.7 m diameter pile under nine ground motions for 2% and 4% longitudinal reinforcement are depicted in Figures 11(a) and 11(b), respectively. For both the reinforcement percentages, plastic hinges are observed near the pile-head only for the near-field earthquakes and Loma Prieta earthquake. It is important to note that the analysis did not yield results for the 0.7 m diameter pile with 0.4% and 1% reinforcement percentages. This observation indicates that the minimum reinforcement criteria according to IRC guidelines might not be adequate for small diameter piles and hence the pile may fail even during small magnitude earthquakes.

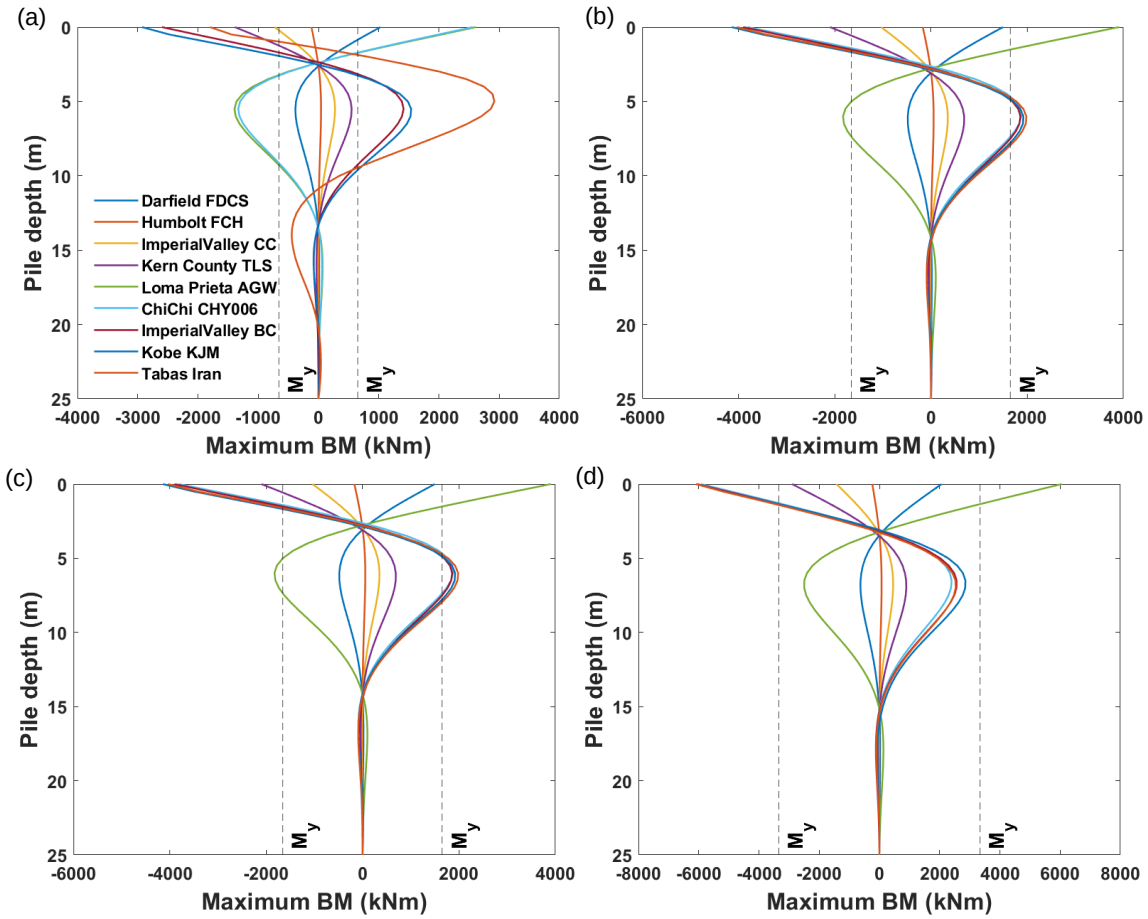

Figure 9. Maximum bending moment profiles of the 1.2 m diameter pile depicting the crossing of the yield moment along the pile length under nine ground motions for (a) 0.4%; (b) 1%; (c) 2%; and (d) 4% longitudinal reinforcement.

Plastic hinge length

Figures 10 and 12 illustrate the regions of the pile that have yielded and shown the nonlinear range of behaviour, which are distinctly highlighted in red. Through these visuals, the plastic hinge zones are clearly identifiable. Notably, only half of the pile lengths are depicted, as the other half indicates no presence of a plastic hinge. The first plastic hinge length, L_{p1} and the second plastic hinge length, L_{p2}, for both 1.2 m and 0.7 m diameter piles extracted from the dynamic analyses considering nine ground motions are tabulated in Table 2. In this research, the plastic hinge lengths obtained from the dynamic analyses have been compared to those recommended by IRC:112.

IRC 112 (2011) identifies three potential locations for plastic hinges along the pile: near the pile head, at the point of maximum BM, and at the interface of soil layers. The code recommends to provide confinement reinforcement over a span of three times the pile diameter along the vertical length at the pile head. Similarly, at the point of maximum BM, it prescribes confinement reinforcement over a span of two pile diameters on each side of this location. If these two locations are considered as the locations where the first and second plastic hinges develop, the prescribed lengths of the plastic hinges, L_{p1} and L_{p2}, according to IRC:112 would amount to 3.6 m and 4.8 m, respectively.

From the dynamic analyses, L_{p1} was found to be in the range of 0.5 to 2 m for different far-field and near-field earthquakes (Table 2) for both 1.2 m and 0.7 m diameter piles. This suggests that the IRC recommendations align more conservatively concerning the length of the first plastic hinge. On the contrary, L_{p2} was found to be in the range of 6 to 7.5 m for the 1.2 m diameter piles with 0.4% longitudinal reinforcement, exceeding the prescribed plastic hinge length. However, for piles with 1% longitudinal reinforcement, L_{p2} ranges from 1.5 to 2 m, which are well within the prescribed limit. It is also important to note that for both 1.2 m and 0.7 m diameter piles with 2% and 4% longitudinal reinforcement, no second plastic hinge was observed.

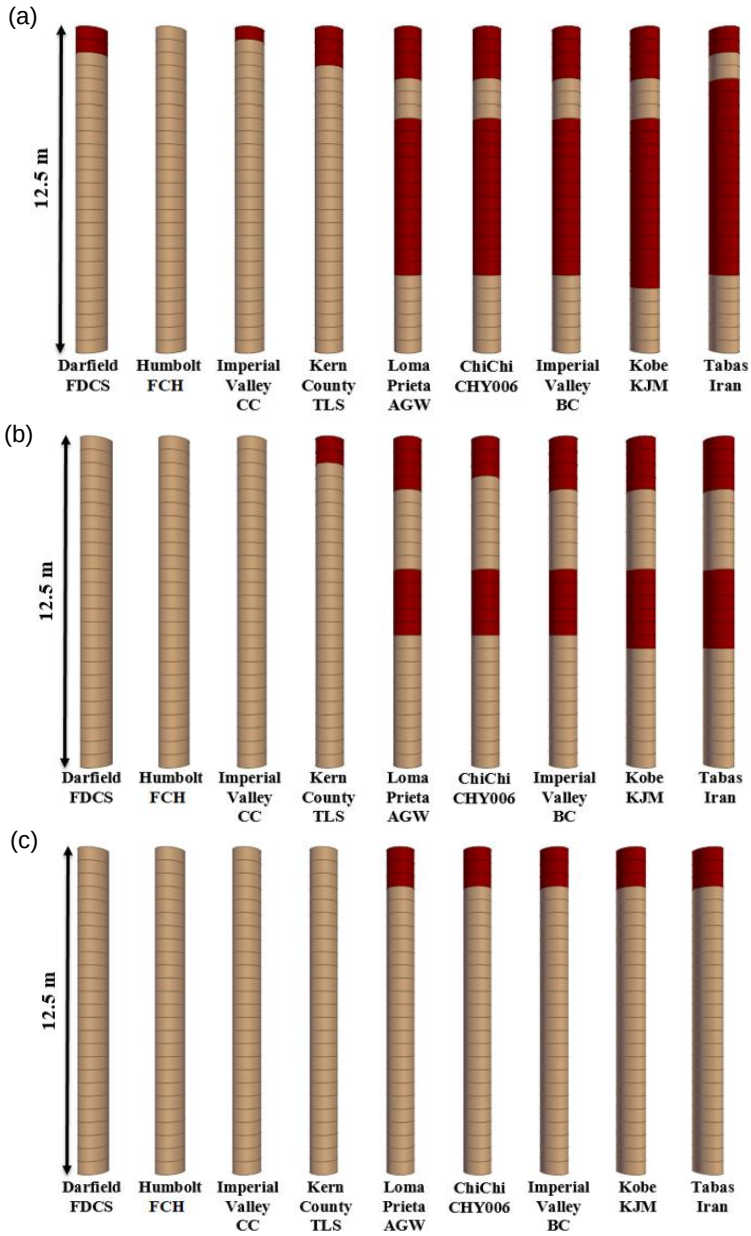

Figure 10. Plastic hinge zone along the pile length for (a) 0.4%; (b) 1%; (c) 2% and 4% longitudinal reinforcement, for the 1.2 m diameter pile.

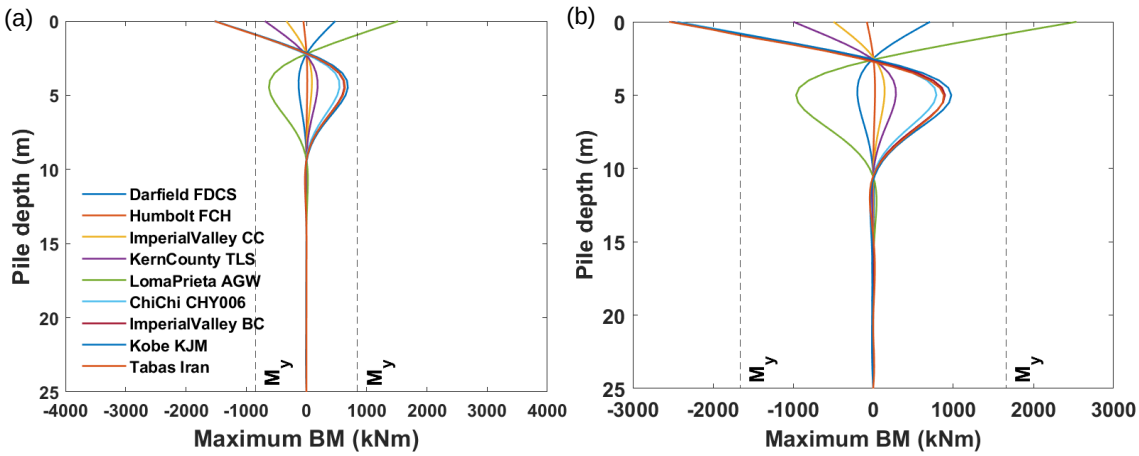

Figure 11. Maximum bending moment profiles of the 0.7 m diameter pile depicting the crossing of the yield moment along the pile length under nine ground motions for (a) 2%; and (b) 4% longitudinal reinforcement.

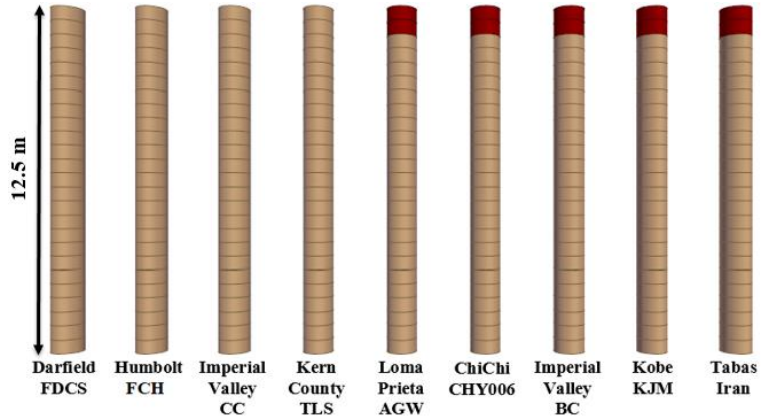

Figure 12. Plastic hinge zone along the pile length for 2% and 4% longitudinal reinforcement for the 0.7 m diameter pile.

Table 2. Observed plastic hinge lengths in the piles under the different ground motions

Earthquakes	1.2 m dia. pile						0.7 m dia. pile	
	0.4 %		1 %		2 % and 4 %		2 % and 4 %	
	L_{p1} (m)	L_{p2} (m)	L_{p1} (m)	L_{p2} (m)	L_{p1} (m)	L_{p2} (m)	L_{p1} (m)	L_{p2} (m)
Darfield FDCS	1	-	-	-	-	-	-	-
Humbolt FCH	-	-	-	-	-	-	-	-
Imperial Valley CC	0.5	-	-	-	-	-	-	-
Kern County TLS	1.5	-	-	-	-	-	-	-
Loma Prieta AGW	2	6	2	2.5	1.5	-	1	-
Chi Chi CHY006	2	6	1.5	2.5	1.5	-	1	-
Imperial Valley BC	2	6	2	2.5	1.5	-	1	-
Kobe KJM	2	6.5	2	3	1.5	-	1	-
Tabas, Iran	1	7.5	2	3	1.5	-	1	-

7. Conclusions

Dynamic analyses have been performed to evaluate the influence of ground motion characteristics, longitudinal reinforcement percentages and pile diameter on the response of single fixed-head piles in homogeneous loose sand profile. A two-step process has been adopted in the analysis where firstly, the free-field motions are evaluated considering nonlinear site response analyses and secondly, dynamic analysis of the pile is carried out by applying these displacement time histories to the soil-end nodes of the springs.

The following conclusions may be drawn from this study:

- The response of the pile under Loma Prieta earthquake (with lesser PHA), which is classified as a far-field earthquake is similar to the near-field earthquakes. This suggests that the classification of ground motions as far-field or near-field based solely on epicentral distances might be insufficient.
- For small diameter piles, the minimum reinforcement criteria according to IRC guidelines may prove inadequate, potentially leading to pile failure even during small magnitude earthquakes.
- Plastic hinge lengths obtained from the dynamic analyses are well within the limit of IRC guidelines for the piles with higher longitudinal reinforcement percentages. However, for the minimum reinforcement of 0.4%, the length of the second plastic hinge which develops below the ground level near the local maximum BM, surpasses the prescribed limit.
- The plastic hinge length in a single pile is influenced by longitudinal reinforcement and pile diameter. Codal recommendations for plastic hinge lengths should account for these parameters while recommending the plastic hinge length for piles.

8. References

American Petroleum Institute (API). (2000). *Recommended practice for planning, designing, and constructing fixed offshore platforms*. API recommended practice 2A-WSD (RP 2AWSD), 21st edition, API.

Baker, J.W. (2007). Quantitative classification of near-fault ground motions using wavelet analysis. Bulletin of the seismological society of America, 97(5), pp.1486-1501.

Boulanger, R.W., Curras, C.J., Kutter, B.L., Wilson, D.W. and Abghari, A. (1999). Seismic soil-pile-structure interaction experiments and analyses. *ASCE Journal of geotechnical and geoenvironmental engineering*, *125*(9), pp.750-759.

Budek, A.M., Priestley, M.J.N. and Benzoni, G. (2000). Inelastic seismic response of bridge drilled-shaft RC pile/columns. *ASCE Journal of structural engineering*, *126*(4), pp.510-517.

Chai, Y.H. (2002). Flexural strength and ductility of extended pile-shafts. I: Analytical model. *ASCE Journal of structural engineering*, *128*(5), pp.586-594.

Chopra, A.K. and Chintanapakdee, C. (2001). Comparing response of SDF systems to near-fault and far-fault earthquake motions in the context of spectral regions. *Earthquake engineering & structural dynamics*, *30*(12), pp.1769-1789.

Filippou, F. C., Popov, E. P., and Bertero, V. V. (1983). Effects of bond deterioration on hysteretic behaviour of reinforced concrete joints. 137-147.

Gohl, B. (1991). *Response of pile foundations to simulated earthquake loading: experimental and analytical results*, Ph.D. Dissertation, University of British Columbia.

Heidari, M. and Hesham El Naggar, M. (2018). Analytical approach for seismic performance of extended pile-shafts. *ASCE Journal of Bridge Engineering*, *23*(10), p.04018069.

IRC 112:2011. *Code of practice for concrete road bridges*, Indian Road Congress.

IS 456:2000. *Plain and reinforced concrete – Code of practice,* Bureau of Indian Standards (BIS).

IS 2911-1-2:2010. *Design and construction of pile foundations, Part 1: Concrete piles, Section 2: Bored Cast in-situ concrete piles*, Bureau of Indian Standards (BIS).

McKenna, F. (2011). OpenSees: a framework for earthquake engineering simulation. *Computing in Science & Engineering*, *13*(4), pp.58-66.

Murchison, J.M. and O'Neill, M.W. (1984). Evaluation of $p-y$ relationships in cohesionless soils. *ASCE In Analysis and design of pile foundations*, (pp. 174-191).

Park, R., Priestley, M.N. and Gill, W.D., 1982. Ductility of square-confined concrete columns. *ASCE Journal of the structural division*, *108*(4), pp.929-950.

Center, P.E.E.R. (2013). PEER ground motion database, *https://ngawest2.berkeley.edu/*.

Priestley, M. J. N., Seible, F., and Calvi, G. M. (1996). *Seismic design and retrofit of bridges*, Wiley-Interscience, New York.

Scott, B.D., Park, R. and Priestley, M.J., 1982, January. Stress-strain behaviour of concrete confined by overlapping hoops at low and high strain rates. In *Journal Proceedings* (Vol. 79, No. 1, pp. 13-27).

Song, S.T., Chai, Y.H. and Hale, T.H. (2005). Analytical model for ductility assessment of fixed-head concrete piles. *ASCE Journal of Structural Engineering*, *131*(7), pp.1051-1059.

SP 16:1980. *Design Aids for reinforced concrete to IS 456:1978,* Bureau of Indian Standards (BIS).